Available online at www.sciencedirect.com

SCIENCE DIRECT

Developmental Biology 278 (2005) 208–219

DEVELOPMENTAL BIOLOGY

www.elsevier.com/locate/ydbio

Mutations in *connexin43* (*GJA1*) perturb bone growth in zebrafish fins

M. Kathryn Iovine[a,*], Emmett P. Higgins[a], Anna Hindes[b], Brian Coblitz[b], Stephen L. Johnson[b]

[a]*Lehigh University, 111 Research Drive, Iacocca B-217, Bethlehem, PA 18015, USA*
[b]*Department of Genetics, Washington University, School of Medicine, 4566 Scott Avenue, St. Louis, MO 63110, USA*

Received for publication 3 June 2004, revised 8 October 2004, accepted 4 November 2004
Available online 26 November 2004

Abstract

Mechanisms that regulate the size and shape of bony structures are largely unknown. The molecular identification of the fin length mutant *short fin* (*sof*), which causes defects in the length of bony fin ray segments, may provide insights regarding the regulation of bone growth. In this report, we demonstrate that the *sof* phenotype is caused by mutations in the *connexin43* (*cx43*) gene. This conclusion is supported by genetic mapping, reduced expression of *cx43* in the original *sof* allele (sof^{b123}), identification of missense mutations in three ENU-induced alleles, and by demonstration of partially abrogated *cx43* function in sof^{b123} embryos. Expression of *cx43* was identified in cells flanking the germinal region of newly growing segments as well as in the osteoblasts at segment boundaries. This pattern of *cx43* expression in cells lateral to new segment growth is consistent with a model where *cx43*-expressing cells represent a biological ruler that measures segment size. This report identifies the first gene identification for a fin length mutation (*sof*) as well as the first connexin mutations in zebrafish, and therefore reveals a critical role for local cell–cell communication in the regulation of bone size and growth.

Keywords: Fin growth; *connexin43*; Gap junctions; *short fin*; Zebrafish; Bone growth

Introduction

The vertebrate skeleton consists of bones of various morphologies, yet the mechanisms controlling the size and shape of bones remain poorly understood. The molecular identification of mutations that result in defects in bone morphology may provide insights regarding underlying mechanisms controlling bone size and shape. Recently, oculodentodigital dysplasia (ODDD), a human syndrome causing craniofacial and limb skeletal malformations, was shown to be caused by mutations in *GJA1* or *connexin43* (*cx43*, Paznekas et al., 2003). Mechanisms for how mutations in a connexin gene might lead to defects in bone morphology are not immediately clear.

Connexins are the subunits of gap junctions, protein complexes that permit the exchange of small molecules (<1200 Daltons) between neighboring cells. Six connexin subunits assemble into a connexon, and two connexons from adjacent cells dock at the plasma membrane to form a proteinaceous channel, or gap junction channel. To date, 21 different connexin genes have been identified in humans (Sohl and Willecke, 2004), with subsets of connexin genes expressed in different tissues. Thus, it has been suggested that this large number of connexin genes accommodates subtle differences in requirements for gap junctional communication among different tissues (White, 2003). Indeed, mutations in different connexin genes cause distinct developmental defects in humans including deafness, skin disorders (*GJB2*/Cx26, Bergoffen et al., 1993; Kelsell et al., 1997, respectively), peripheral neuropathies (*GJB1*/Cx32, Bergoffen et al., 1993), and cataracts (*GJA8*/Cx50, Shiels et al., 1998). While the precise role that gap junctions play during development and morphogenesis is not clear, the identification of mutations in connexin genes resulting in disease supports a crucial function of gap junctions during development, homeostasis, and tissue function. As such, the molecular identification of lesions in *cx43* that cause ODDD suggests that gap junctional intercellular communication (GJIC) is required during mammalian bone morphogenesis.

* Corresponding author. Fax: +1 610 758 4004.
E-mail address: mki3@lehigh.edu (M.K. Iovine).

0012-1606/$ - see front matter © 2004 Elsevier Inc. All rights reserved.
doi:10.1016/j.ydbio.2004.11.005

We utilized the properties of the zebrafish fin skeleton to examine the growth and development of vertebrate bone. Fins are comprised of segmented fin rays whose length depends on the number and size of bony segments (Iovine and Johnson, 2000). Fin rays contain several tissues in the mesenchymal compartment including bone, nerves, blood vessels, and undifferentiated cells, together surrounded by an overlying epithelium. Growth occurs by the distal addition of bone segments (Goss and Stagg, 1957; Haas, 1962) and requires cell proliferation of the distal-most undifferentiated cells (Goldsmith et al., 2003). Recently divided cells cross actinotrichia (i.e., elastoidin fibrils that emanate from the distal basal epithelium and lay alongside bone matrix or lepidotrichia) and condense as osteoblasts. Thus, actinotrichia form a boundary between differentiated cells (i.e., osteoblasts) and the germinal region of undifferentiated cells undergoing cell division (Mari-Beffa et al., 1989). Bone formation in the fin occurs by the direct ossification of bone matrix (intramembranous ossification) without passage through a cartilaginous precursor (Landis and Geraudie, 1990). While some of the cellular changes that occur during fin growth have been examined, the mechanisms that control the addition and growth of new segments are not understood. Interestingly, fin length mutants have been identified which affect segment number (*long fin*, Iovine and Johnson, 2000 and *rapunzel*, Goldsmith et al., 2003) or segment length (*short fin*, Iovine and Johnson, 2000). Thus, a genetic approach may be taken to identify underlying mechanisms which regulate fin length. In order to reveal the mechanisms that regulate bone growth and morphology, we sought the molecular identification of *short fin* (*sof*^{b123}). Here, we report that the *sof*^{b123} phenotype is caused by hypomorphic mutations in the gap junction channel protein, Cx43. The pattern of *cx43* expression along the length of newly forming segments during fin growth suggests a model where local cell–cell communication functions as a biological ruler that is able to regulate bone size.

Materials and methods

Fish rearing

Wild-type fish stocks used for this study were from the C32 strain (Rawls et al., 2003). *sof*^{b123} was also in the C32 background. Zebrafish were raised at constant temperature of 25°C with 14 light: 10 dark photoperiod (Westerfield, 1993).

Mapping

We localized the *sof*^{b123} mutation to LG20 by centromere-linkage analysis (Johnson et al., 1996) using simple sequence repeat markers (SSR, Shimoda et al., 1999) by early pressure of *sof*^{b123}/+^{SJD} oocytes. SSR markers previously localized to the vicinity of the *sof*^{b123} mutation were then utilized to finely map the *sof*^{b123} mutation in *sof*^{b123}/+^{SJD} × *sof*^{b123} crosses. Two panels that segregated *sof*^{b123} were tested. One panel of 576 individuals segregated *sof*^{b123} only. In the second panel, recombinants in approximately 5 cM interval between *sof*^{b123} and the distal pigment pattern mutation, *transparent* (*tra*), were first selected from a total of 880 individuals (resulting in increased mapping resolution in this interval). In addition to mapping with respect to SSR markers, we also developed single nucleotide polymorphism (SNP) markers from genes localized to this region (Hukriede et al., 2001) or developed additional SSR markers using the whole genome shotgun and clone sequence (http://www.ensembl.org/Danio_rerio). A description of these markers and the respective polymorphisms may be found in Table 1.

Non-complementation screen

SJD males were mutagenized using the chemical mutagen N-ethyl-N-nitrosourea (ENU) by allowing males to swim in 3 mM ENU solution for three 1-h periods over the course of 6 weeks. Eggs from *sof*^{b123} homozygous females were fertilized in vitro using sperm from mutagenized males. F1 progeny were raised until it was possible to identify small fins, approximately 10–12 weeks. We identified putative new alleles of *sof*^{b123} with a frequency of approximately 1:500 adult animals screened. Founder animals with short fins were back-crossed to *sof*^{b123} to confirm a single locus was responsible for the *short fin* phenotype, and out-crossed to C32 in order to isolate the new allele. Carriers for the mutation at the SJD haplotype were identified by PCR using the flanking SSR markers z63495 and z3954 (Shimoda et al., 1999). Three new ENU-induced alleles were isolated.

Sequencing

Sequencing was completed using a 3100 Genetic Analyzer (Applied Biosystems). A single exon containing the entire coding sequence of zebrafish *cx43* was amplified from SJD, C32, *sof*^{b123}, *sof*^{j7e1}, *sof*^{j7e2}, and *sof*^{j7e3} genomic DNA using the polymerase chain reaction. Both strands of the coding region were sequenced. In addition to the identified mutations we also found two synonymous changes in the SJD inbred line. These two synonymous polymorphisms were found in all three alleles isolated on the SJD haplotype (Table 2).

Morphometry

For segment length measurements, fish were first anesthetized in Tricane (Westerfield, 1993). Measurement

Table 1
Markers used in *sof*^{b123} positional cloning

Marker[a]	WGS assembly (v4)[b]	PCR or sequencing primers[c]	Polymorphism type[d]	Polymorphism
z20046	20:50.340	F-TTCAGGTTTAAGGTTATAAAACGA	size	SJD: 175 bp
		R-AACCAATATGTCATGGCATCC		*sof*: 160 bp
85g10y	20:50.478	F-AGATGCAGATGGAAACTGAC	SNP	SJD: TC**T**ATC at approximately 54 bp
		R-CATGCAAATATGTGCTCACT		*sof*: TC**C**ATC at approximately 54 bp
2921	20:50.531	F-ATGGTTCGAAAATGAGAAAA	size	SJD: 590 bp
		R-TGCTGAGAAAATGACAATGA		*sof*: 620 bp
33642	20:50.688	F-TGGGCACTTCTTACTTAACC	plus/minus	SJD: present (500 bp)
		R-TGAAATGTTCATAGCACAACA		*sof*: absent
128311	20:50.724	F-CTGACGTCTTTGTTTTCCTC	SNP	SJD: CC**T**TCA at approximately 417 bp
		R-GCAATAACAAACTCCCACAT		*sof*: CC**A**TCA at approximately 417 bp
71570	20:50.732	F-ACTTTTACACAGCTCCTTGC	SNP	SJD: AT**G**TAT at approximately 381 bp
		R-CCAAACTGGGTACAGGTCTA		*sof*: ATATAT at approximately 381 bp
35877	20:50.762	F-CTGCTGTTTAAAATCCAAGC	SNP	SJD: TTC**T**GG at approximately 233 bp
		R-ATGTCTGTGCATGAAGATCA		*sof*: TTC**C**GG at approximately 233 bp
wz8407	20:50.781	F-CGTTTTTGTTTGGGATTGCT	insertion	SJD: no insertion
		R-TATATGCCAGCGTAGCTCCA		*sof*: TGTG at approximately 159 bp
ctg601L3	20: 50.827	F-AACGAACATACAAACGGACT	size	SJD: 250 bp
		R- CCCTCTGTAGTGAGAAGCTG		*sof*: 500 bp
601L11	20:50.993	F-TCATCTTGAAATGAGGCTGT	size	SJD: 500 bp
		R-TTGATTCTCGGTAGGAGAGA		*sof*: 560 bp
z63495	20:51.121	F-ACCTAATAAAGTGGCCGGTG	size	SJD: 120 bp
		R-TGGATAACCTCTTCGGTTCG		*sof*: 190 bp

[a] Markers beginning with "z" are from Shimoda et al. (1999). Other markers were developed from Sanger Institute's Zebrafish Whole Genome Shotgun Assembly (names reflect sequence assemblies, contigs or BAC ends from V2 or V3 assembly) or from WashU Zebrafish EST Assemblies (see zfish.wustl.edu).
[b] Position of markers on the V4 Whole genome shotgun assembly. Positions 50,474,800 to 51,121,000 on this assembly are from sequenced BAC clones, except for 50,740,499 through 50,782,566. For our analysis, we replaced this 32 kb region with nucleotides 1 – 57,145 from a more recently sequenced BAC clone (**CR352322**), which includes the 6 connexin genes discussed here.
[c] For sequencing, we used the forward (F) primer.
[d] Size polymorphisms were assessed on 1.5% agarose gels, SNPs or small insertions were assessed by sequencing reads.

of body length, fin length, and segment length has been described previously (Iovine and Johnson, 2000). All measurements were made by using a Nikon SMZ800 stereomicroscope fitted with a calibrated eyepiece reticule.

In situ hybridization

Riboprobe synthesis using digoxigenin-labeled UTP and in situ hybridization were performed as described elsewhere (Poss et al., 2000). Two probes were used to insure that *cx43* expression was specifically detected. One probe was generated by amplification of the coding sequence of *cx43* and used as template for riboprobe synthesis. (F-5′GCTAGAACTCCCTCAAGATGG 3′; RT7-5′TAATACGACTCACTATAGGGTCCTCTA-GCGTTGGGATGTGG 3′). Since the reverse oligo contains a binding site for T7 RNA polymerase, the amplified product was used directly as template for the riboprobe (the underlined portion of the reverse oligo is *cx43*-specific). The second probe was generated similarly, but the template sequence was amplified from the 3′UTR of *cx43* (F-5′CCATGCCACATCCCAACG 3′; RT7-5′ TAATAC-GACTCACTATAGGGTGCTGATGAACGTATTGC 3′). Both probes result in similar expression patterns in fins and embryos. To prevent melanin synthesis and facilitate analysis of *cx43* expression in 72 hpf animals, embryos were treated with 0.1 mM phenylthiourea (PTU) as per Rawls and Johnson, 2000 (except that water containing PTU was changed daily).

Cryosectioned fins were first processed for in situ hybridization, post-fixed in 4% paraformaldehyde in PBS and washed in PBS before embedding in 1.5% agarose, 5% sucrose. Blocks were soaked in 30% sucrose overnight or until sinking. Sections (16 μ) were cut on a Leica cryostat and collected on Superfrost microscope slides.

RT-PCR analysis

RT-PCR was completed on 72 hpf hearts, adult hearts, and 72 hpf embryos. Total RNA was isolated from adult and embryonic tissues using Trizol (Invitrogen). For RT-PCR of 72 hpf embryonic hearts, hearts were dissected using fine needles and then immediately placed in Trizol reagent (5 hearts in 100 μl Trizol). SuperScript II reverse transcriptase (Invitrogen) in combination with an oligo dT primer were used to generate total cDNA from approximately 5 μg of RNA. PCR was completed with Eppendorf Taq polymerase. The 3′UTR of *cx43* mRNA was amplified using the primers described above (see in situ hybridization probes). Primers which amplify *collagen 1a* (*col-1a*, F-CCC TGC TGG AAA GAC TGG; R-TGA TTA GGT GCA CCA ACG TCC) were used to demonstrate that the dissected hearts were not contaminated with surrounding tissue.

Morpholino injections

The morpholino antisense oligonucleotide "*cx43*-MO" (5′-TTC CCA ACG CAC TCC AGT CAC CCA T 3′) was designed against the *cx43* translational start site and purchased from Gene Tools, LLC. The standard control morpholino (5′-CCT CTT ACC TCA GTT ACA ATT TAT A 3′) was purchased from Gene Tools, LLC, and does not target zebrafish genes (http://198.88.150.227/genetools/ordering/products.aspx#standard). Wild-type or homozygous *sof*^{b123} embryos primarily at the 1-cell stage (with chorion intact) were injected with approximately 2 nl of stocks ranging from 20 to 100 μM of morpholino diluted in Danieau's solution.

Staining for globin expression

Staining for expression of globin was completed as described (Detrich et al., 1995). Briefly, dechorinated, non-fixed embryos at 72 hpf were stained for 15 min in the dark in 0.6 mg/ml *o*-dianisidine, 0.01 M sodium acetate, pH 4.5, 0.65% H_2O_2, and 40% (vol/vol) ethanol and examined on a Nikon SMZ1500 microscope.

Detection of proliferating cells using BrdU

Labeling was completed by allowing 10 wild-type or *sof*^{b123} homozygous fish (10 weeks of age) to swim in 50 μg/ml BrdU made in fresh water for 6 h. Fins were harvested and fixed in 4% paraformaldehyde in PBS before processing for BrdU. Detection on whole mount fins was completed as described (Nechiporuk and Keating, 2002). Briefly, fins were dehydrated in 100% methanol and then gradually rehydrated in a methanol series containing PBTx (PBS, 0.1% Triton X-100). Fins were treated with 2N HCl in PBTx for 30 min at room temperature and then blocked with 0.25% BSA in PBTx for 1–2 h. A mouse monoclonal antibody against BrdU (Roche) was diluted 1:50 in blocking solution and incubated with fins overnight at 4°C. Extensive washes were completed in PBTx (last wash in blocking solution). An anti-mouse antibody conjugated to Alexa-546 (Molecular Probes) was diluted 1:200 in blocking solution and incubated with fins overnight at 4°C. Extensive washes were completed prior to mounting in Vectashield. Labeled cells were visualized and counted using a Nikon Eclipse E800 compound microscope. Cells were counted only from the distal portion of the third fin ray in either lobe (typically the longest fin ray).

Results and discussion

The sof phenotype is caused by mutations in zebrafish cx43

We first mapped the *sof*^{b123} mutation to zebrafish linkage group 20 (LG20) by half-tetrad centromere linkage (not shown, Johnson et al., 1996). The *sof*^{b123} mutation was next mapped on two panels of 1456 meioses to a 1.3 cM region between SSLP markers z20046 and z63495 (Fig. 1A). In order to develop the map further and to identify candidate genes, we screened ESTs and genes localized on the zebrafish transcript maps (Hukriede et al., 2001). We identified a gene with zero recombination events to *sof*^{b123} indicating close physical proximity. This gene has been shown to be orthologous to human *GJA1*, or *connexin43* (*cx43*, Cheng et al., 2003). To develop the physical map, we used the sequence of zebrafish *cx43* and the flanking markers, z20046 and z63495. This was initially achieved by comparing these sequences to the whole genome shotgun assembly (Sanger Institute, assembly version 2). We identified sequence contigs containing these markers, which were in turn associated with fingerprinted BAC clone (fpc) contigs. Using the BAC end sequences associated with the fpc contig, we were able to order the contigs in this region and develop SSLP markers (see Table 1). Subsequent versions of the sequence assembly (assembly version 4, or v4) have now nearly completely contiguated the *sof* critical region with sequenced BAC clones (Chr20 from 50.478 to 51.121 Mb). The sole remaining gap in this region is remediated by replacing the whole shotgun assembly sequence from nucleotides 50,740,499 to 50,782,556 with nucleotides 1–57,145 from the BAC clone zK261A18 (**CR352322**).

We identified genes in the critical region by examining the Ensembl Contig Viewer for this region (http://www.ensembl.org/Danio_rerio/) or by BLAST comparison of the replacement region (for which there is no Ensembl Contig View) against the NCBI non-redundant protein database and the zebrafish EST database. This identified eight genes in the critical interval (from marker 2921 at position 50,530,900 to marker 610L3 at position 50,827,100): the zebrafish ortholog of human *C6orf170*, a steroid dehydrogenase (*sdh*), and six connexins (including the zebrafish ortholog of human *cx43*). Interestingly, the replaced sequence from the whole genome shotgun assembly shows only four connexin genes (and lacks *cx43*). The replacement clone (**CR352322**) clearly shows six connexin genes for this region (including *cx43*). Thus, the independent assignment of *cx43* to this region by meiotic mapping (above) strongly supports the inclusion of this replacement sequence over the whole genome shotgun assembly sequence.

Phylogenetic comparison of this cluster of six LG20 connexin genes reveals that they are related (Fig. 1B). However, only one of these connexin genes, the gene previously described as the mammalian *cx43* ortholog (Cheng et al., 2003), is clearly orthologous to mammalian *cx43*. The remaining five neighboring connexin genes do not exhibit clear orthology to *cx43* or to two closely related mammalian connexins. Since these genes do not exhibit clear orthologous relationships to mammalian connexins and their function is uncharacterized, we refer to these

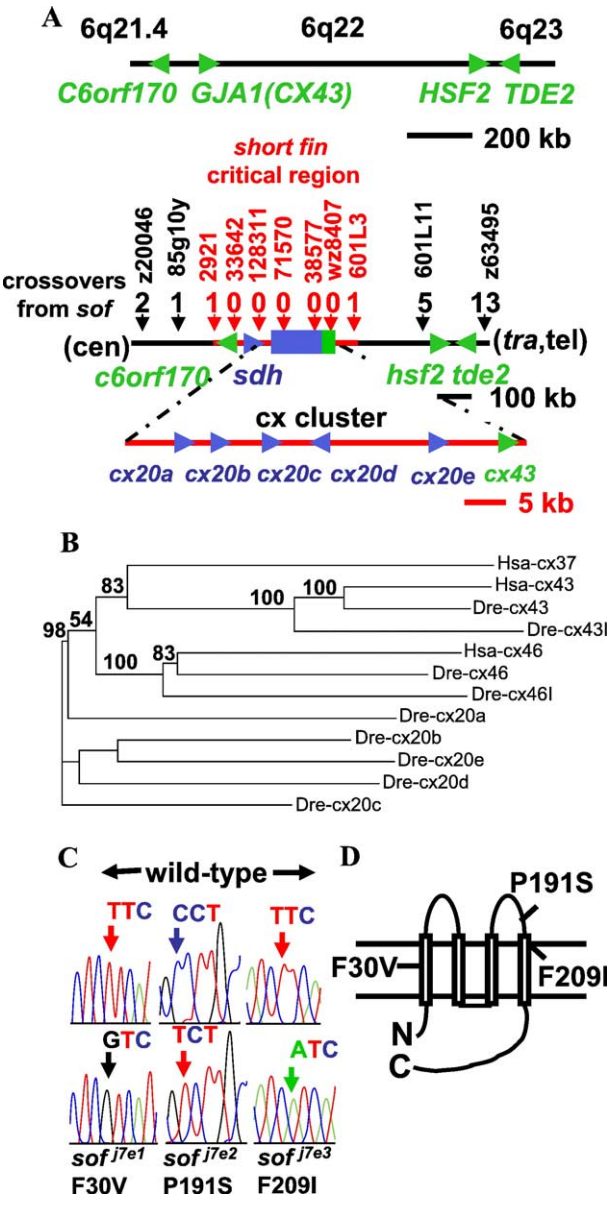

Fig. 1. Map of the *sof*^{b123} region. (A) (top) Syntenic region of human chromosome 6. (bottom) Meiotic map representing approximately 700 kb of contiguous sequence of the *sof*^{b123} region. Red lines represent the region spanning the *sof*^{b123} critical interval, markers in red are contained in the critical interval. SSLP markers were developed and named based on the sequence assembly or contig names from the zebrafish v2 and v3 whole genome shotgun assemblies (http://www.sanger.ac.uk/Projects/D_rerio/), or from EST sequence assemblies (http://zfish.wustl.edu/). See Table 1 for more details regarding marker descriptions and the physical positions of each marker on the approximately 700 kb of contiguous sequence spanning *sof*^{b123}. (B) A phylogram of the connexin genes related to zebrafish *cx43* was generated using ClustalW. A neighbor-joining bootstrap analysis was conducted in PAUP* (Swofford, 2000) based on standard distances (mean character difference). Bootstrap values were estimated from 1000 replicates; values greater than 50% are shown on the tree. Accession numbers for the amino acid sequences used in this comparison may be found in Table 2. (C) Electrophoretograms showing the mutations identified in coding sequence from the three ENU-induced *sof* alleles. (D) Cartoon of a single connexin protein in a double-lipid bilayer. The location of each ENU-induced lesion is indicated. N indicates amino terminus, C indicates carboxy terminus (both intracellular).

connexin genes based on their associated linkage group (LG20; *cx20a*, *cx20b*, etc.).

Comparison of this region to the corresponding region in human reveals considerable conservation of synteny. Four human genes are found in a 1.6-MB span on human chromosome 6 in the same order as zebrafish (*C6orf170*, *GJA1*/*cx43*, *HSF2*, and *TDE2*). The human region (as well as the human genome) lacks an orthologous steroid dehydrogenase and the five additional connexin genes. Since the five connexin genes in this region appear related, are physically close together, and are not orthologous to mammalian connexin genes, one possibility is that these genes arose from several gene duplication events in the zebrafish lineage. Alternatively, perhaps these five connexin genes arose initially on the ancestral chromosome and were lost more recently in the mammalian lineage.

Of the eight candidate genes in the *sof*^{b123} critical interval, only *cx43* is identified among the 33,000 fin ESTs (SLJ, unpublished data), revealing *cx43* as a strong candidate for *sof*^{b123}. Of the others, *sdh* (4 ESTs), *cx20c* (5 ESTs), and *cx20b* (20 ESTs) are identified among the remaining approximately 500,000 zebrafish ESTs, providing evidence that these genes are expressed and function in tissues other than fins. In contrast, *c6orf170* (0 ESTs), *cx20a* (1 EST), *cx20d* (0 ESTs), and *cx20e* (0 ESTs) identify one or zero ESTs, providing little support that these sequences are genes, and raising the possibility that these sequences represent pseudogenes. Based on this analysis of the predicted expression of the candidate genes in the *sof*^{b123} critical interval, we chose to analyze *cx43* in more detail.

We sequenced the coding region of *cx43* from the original allele (*sof*^{b123}) as well as three non-complementing alleles induced by N-ethyl-N-nitrosourea (ENU, *sof*^{j7e1},

Table 2
Accession numbers for connexin sequences related to zebrafish *cx43*

Name	Accession[a]	CDS derived from CR352322[b]		
		Start	Stop	Strand
Hsa-cx37	AAH72389	N/A	N/A	N/A
Hsa-cx43	AAH26329	N/A	N/A	N/A
Hsa-cx46	AAD42925	N/A	N/A	N/A
Dre-cx20a	N/A	562	1458	+
Dre-cx20b	NP_955906.1	4182	5039	+
Dre-cx20c	N/A	11866	12627	+
Dre-cx20d	N/A	18982	18239	-
Dre-cx20e	AAQ17184	33831	34644	+
Dre-cx43	NP_571113	41046	42191	+
Dre-cx43l	ENSDARP00000022711	N/A	N/A	N/A
Dre-cx46	AAM76069	N/A	N/A	N/A
Dre-cx46l	NP_997991	N/A	N/A	N/A

Predicted protein sequences for *Dre-cx20a*, *Dre-cx20c*, *Dre-cx20d*, and *Dre-cx43l* may also be found in supplementary materials.

[a] Accession numbers are for protein sequences. For *Dre-cx43l*, the only available accession number is through the Ensembl database.

[b] For all six LG20 connexins, predicted protein sequences may be derived from BAC clone sequence using 'start' and 'stop' nucleotides positions shown.

sof^{j7e2}, *sof*^{j7e3}). Missense mutations were identified in each of the ENU-induced alleles from the *cx43* coding sequence (Fig. 1C). Two of these alleles have lesions in the transmembrane domains, F30V (*sof*^{j7e1}) and F209I (*sof*^{j7e3}). A third allele is found in the second extracellular loop (*sof*^{j7e2}, P191S), which may be important for connexon to connexon docking at the plasma membrane. The location of these lesions in the channel region suggests that GJIC through *cx43* gap junctions may be affected (Fig. 1D). No lesion was found in the coding sequence of *cx43* from the original, spontaneous allele, *sof*^{b123}. However, expression levels of *cx43* were significantly reduced in *sof*^{b123} animals (below and Fig. 3B), suggesting that the mutation in the original allele affects the abundance of *cx43* mRNA. The identification of *cx43* lesions in our three ENU-induced alleles of *sof*, in combination with the reduced expression of *cx43* in *sof*^{b123} animals, strongly supports the conclusion that the *cx43* gene corresponds to the *sof* mutations.

In order to determine the relative severity of each ENU-induced allele compared with *sof*^{b123} animals, we measured segment length in homozygotes, in heterozygotes, and in selected trans-heterozygotes (i.e., ENU-induced allele/original allele). We find that homozygous alleles of *sof*^{j7e1} and *sof*^{j7e2} exhibit segment lengths the same as *sof*^{b123} animals, but homozygous stocks of *sof*^{j7e3} mutants have segments (and fins, not shown) longer than *sof*^{b123} (Table 3). This suggests that the *sof*^{j7e1} and *sof*^{j7e2} alleles are equally as severe as the original allele, and that *sof*^{j7e3} is less severe. The finding that heterozygotes for all of our *sof* alleles (including *sof*^{b123}) have slightly shorter segments than wild-type animals, and that trans-heterozygotes of each ENU-induced allele results in a more severe phenotype than each allele when homozygous argues that all of the *sof* alleles may also exhibit dominant negative activity.

Expression of cx43 during ontogenetic and regenerative fin growth

To further explore how *cx43* expression and function may regulate segment size we examined the expression pattern of *cx43* in growing fins. Caudal fins were harvested from 8-week-old zebrafish and processed for in situ hybridization using a digoxigenin-labeled *cx43* probe (Fig. 2A). Three expression domains were observed. Most distally, we observed expression in a crescent-shaped pattern. Proximal to this crescent, we observed *cx43* expression laterally along the dorsal and ventral border flanking the bone segment germinal region (i.e., the distal mesenchymal region where cell division occurs during segment addition). Finally, *cx43* expression was observed surrounding the most newly formed joint. Both the distal crescent and the joint expression of *cx43* are reminiscent of the expression pattern for *evx1*, a homeobox gene previously shown to be expressed in a subpopulation of osteoblasts (Borday et al., 2001). Cryosectioning revealed that the *cx43* and *evx1* expression patterns are distinct in the distal crescent but are partially overlapping around the joint. Transverse sections through the distal crescent showed that *evx1*-expressing cells are found lateral to the actinotrichia in the region of differentiated osteoblasts (Borday et al., 2001 and Fig. 2A-1′ for schematic). In contrast, sections through *cx43* stained fins revealed that the *cx43*-expressing cells are medial to the actinotrichia (Fig. 2A-1). In the joint, the expression of *cx43* is observed in cells overlying, as well as flanking, the newly forming joint (Fig. 2A-3). Sections reveal that these cells reside adjacent to the outer surface of the bone matrix (not shown, see below for sections of joints during fin regeneration), similar to the location of *evx1*-expressing cells in joints (which are found on both the inner and the outer surfaces of the bone matrix, Borday et al., 2001). Interestingly, *cx43*- and *evx1*-expressing cells are found in different compartments in the distal crescent, but both are identified in subpopulations of osteoblasts surrounding joints. Based on the shared expression pattern in the joints, an attractive possibility is that the expression of *cx43* in the distal crescent identifies a population of undifferentiated precursors in the germinal region which will later give rise to cells that cross the actinotrichia and differentiate as *evx1*-positive joint cells. The unique lateral expression of *cx43* was observed along the dorsal and ventral boundaries of the rows of actinotrichia (Fig. 2A-2), flanking the area where cell proliferation occurs during segment growth. We speculate that the expression of *cx43* in these cells may contribute to the regulation of segment length.

We next examined *cx43* expression in regenerating fins, which typically exhibit increased expression levels over ontogenetically growing fins, in order to facilitate the

Table 3
Segment length in *sof* alleles

Homozygotes		Heterozygotes		Trans-heterozygotes	
Genotype	Segment length (mm)[a]	Genotype	Segment length (mm)[a]	Genotype	Segment length (mm)[a]
sof^{b123}/*sof*^{b123}	0.24 ± 0.02	*sof*^{b123}/+	0.31 ± 0.03	–	–
sof^{j7e1}/*sof*^{j7e1}	0.24 ± 0.03	*sof*^{j7e1}/+	0.32 ± 0.02	*sof*^{b123}/*sof*^{j7e1}	0.21 ± 0.03
sof^{j7e2}/*sof*^{j7e2}	0.24 ± 0.02	*sof*^{j7e2}/+	0.28 ± 0.03	*sof*^{b123}/*sof*^{j7e2}	0.21 ± 0.03
sof^{j7e3}/*sof*^{j7e3}	0.32 ± 0.02	*sof*^{j7e3}/+	0.31 ± 0.03	*sof*^{b123}/*sof*^{j7e3}	0.23 ± 0.02
+/+	0.35 ± 0.03				

[a] Segment length was measured in the most proximal segment from the longest fin ray in the ventral lobe in each of 10 adult fish (typically the third fin ray).

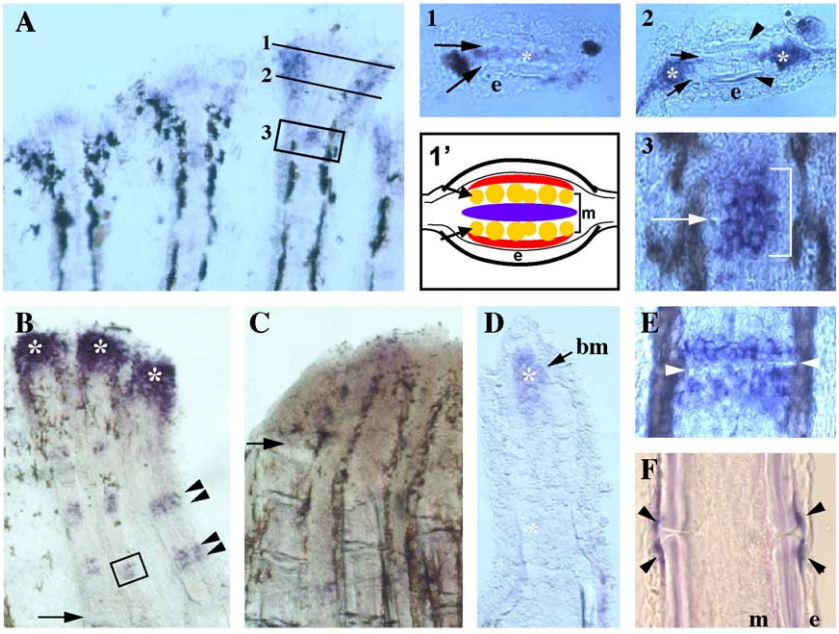

Fig. 2. Expression of *connexin 43* in fins. In situ hybridization was completed using a probe that recognizes the *cx43* coding sequence. (A) Ontogenetically growing fin. Numbers indicate areas of further interest. (1) Transverse section through distal crescent. Arrows, actinotrichia; e, epidermis; *, *cx43*-expressing cells. (1′) Cartoon of transverse section through the distal crescent. Arrows, actinotrichia; e, epidermis; m, mesenchyme. Blue reflects undifferentiated cells medial to actinotrichia. Red represents cells which have crossed actinotrichia and become determined as osteoblasts (i.e., *evx1*-positive cells). (2) Transverse section through lateral *cx43*-stained cells. Arrows, actinotrichia; arrowheads, lepidotrichia; e, epidermis; *, *cx43*-expressing cells. (3) High magnification of a representative young joint, similar to boxed region in A. Arrow points to newly forming joint. Bracket identifies *cx43*-stained cells. (B) Wild-type regenerating fin at 5 dpa. Arrow, amputation plane; arrowheads, *cx43*-stained cells around mature joint; *, *cx43*-expressing cells in the blastema. (C) *sof*^{b123} regenerating fin at 5 dpa. Arrow, amputation plane. (D) Longitudinal cross-section through a *cx43*-stained regenerating fin. The basement membrane (bm) separates the epithelial and mesenchymal compartments. *, *cx43*-expression. (E) High magnification of a representative mature joint, similar to boxed region in B. Arrowheads point to joint. (F) Longitudinal cross-section through a mature joint. Arrowheads, *cx43*-stained cells; e, epidermis; m, mesenchyme.

identification of expressing cells. Expression of *cx43* was apparent as early as 1 day post-amputation (dpa, data not shown). Thereafter, regenerating fins exhibit similarly high expression of *cx43* in the blastema (the population of cells which contributes to new fin outgrowth) as well as along the boundaries of regenerating segments (5 dpa shown in Fig. 2B). This pattern was consistent for all time points examined (3, 5, 8 dpa). Sectioning along the longitudinal axis of stained regenerating fins identified expression in a population of undifferentiated cells in the distal blastema (Fig. 2D) and in a subpopulation of osteoblasts surrounding both newly formed and mature joints (Fig. 2F). Thus, *cx43* expression persists in the older segments during the rapid growth of regeneration, while the *cx43* transcript is not detected in the penultimate segments during ontogeny (Fig. 2A). This difference provides an opportunity to further examine the morphology of more mature joints. High magnification of a mature joint in whole mount revealed *cx43* expression in 2–3 rows of osteoblasts which flank the joint (Fig. 2E), distinguishing the morphology of a mature joint from a newly forming joint (Fig. 2A-3). A similar pattern of *cx43* expression in articulating regions of skeletal elements has been observed in the developing mouse (Chatterjee et al., 2003), suggesting this may represent a conserved function of *cx43*. Importantly, *cx43* expression is barely detectable in *sof*^{b123} regenerating fins (Fig. 2C), correlating the reduction of *cx43* with short fin ray segments.

The sof^{b123} *allele represents a hypomorphic allele of cx43*

Our analysis is consistent with the appropriate identification of mutations in *cx43* being responsible for the *sof*^{b123} phenotype (i.e., short fin ray segments). Still, it was not clear why the *cx43* mutations in zebrafish fail to show the defects, which have been observed for *cx43* deletions in mouse. For example, knockout mutations of *cx43* in the mouse causes conotruncal malformations of the heart resulting in ventricular outflow obstruction and death several hours after birth (Reaume et al., 1995). Further examination of the knockout mouse revealed delayed ossification of both intramembranous and endochondral bone (Lecanda et al., 2000), as well as reduced hematopoiesis (Montecino-Rodriguez and Dorshkind, 2001). One explanation is that the *cx43* alleles described here are hypomorphic, producing sufficient *cx43* function to permit embryonic development but insufficient *cx43* function to permit normal segment morphogenesis. To test this, we monitored expression in *sof* embryos by in situ hybridization. A previous study demonstrated that the *cx43* promoter can drive reporter gene expression in the neural tube, in migrating neural crest cells, and in the developing

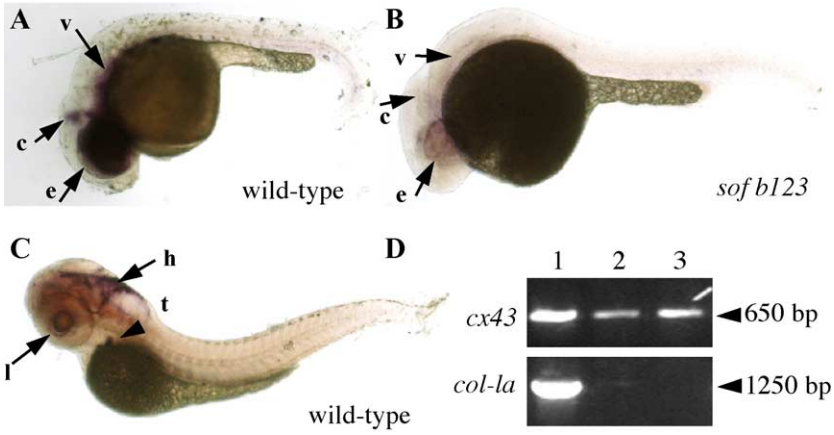

Fig. 3. Expression of *connexin 43* in embryos. In situ hybridization was completed using a *cx43* probe against the *cx43* 3′UTR. (A) Expression of *cx43* in wild-type embryo at 24 hpf. e, eyes; c, cerebellum; v, vasculature. (B) Expression of *cx43* in *sof* embryo at 24 hpf. e, eyes; c, cerebellum; v, vasculature. (C) Expression of *cx43* in wild-type larvae at 72 hpf. Embryos were treated with PTU to prevent the production of melanin and facilitate the identification of stained structures. l, lens epithelium; h, hindbrain; t and arrowhead, thymus. (D) RT-PCR from 72 hpf whole embryos (lane 1), 72 hpf embryonic hearts (lane 2), and adult hearts (lane 3). The top panel shows amplification from *cx43*-3′UTR primers, the bottom panel shows amplification from *col-1a* primers. Approximate sizes of amplified products are shown on the right (arrowhead).

heart at 19 hpf (Chatterjee et al., 2001). Consistent with the reporter gene expression, we observed expression in eyes, cerebellum, and vasculature in 24 hpf embryos (Fig. 3A). At later stages, robust expression of *cx43* becomes limited to the lateral epithelium surrounding the lens (see also Cheng et al., 2003), areas of the hindbrain, and the thymus (Fig. 3C). More sensitive methods of detecting gene expression reveal that *cx43* is expressed in other tissues as well. In particular, RT-PCR of the *cx43* 3′UTR reveals that *cx43* is also expressed in the heart in 72 hpf embryos and adults, even though it is not detectable by whole mount in situ hybridization (Fig. 3D). The expression of *cx43* first in migrating neural crest cells followed by more restricted expression limited to developing organs in later stages is similar to the *cx43* expression pattern observed in mouse and chick (Bao et al., 2004). Examination of *cx43* expression in sof^{b123} mutants confirms that expression is significantly reduced but is not completely absent (Fig. 3C), consistent with sof^{b123} behaving as a hypomorphic allele of *cx43*. A further prediction of the hypothesis that the sof^{b123} mutation is a hypomorph is that sof^{b123} will be more sensitive to *cx43* inactivation via morpholino antisense technology than wild-type embryos.

Morpholino antisense technology prevents translation of the targeted gene and is a reliable method for gene knockdown in zebrafish (Nasevicius and Ekker, 2000). Injection of a standard control morpholino (i.e., a morpholino oligo without gene specificity) permits normal zebrafish development, but injection of a *cx43*-specific morpholino (*cx43*-MO) results in severe phenotypes reminiscent of the phenotypes observed in the $cx43^{-/-}$ mouse (Table 4). When a moderately high dose of *cx43*-MO is injected (approximately 1.5 ng), we find defects in heart folding, reduced hematopoiesis, and less frequently, small eyes. More than one of these phenotypes is typically apparent in affected individuals. Most often, heart and hematopoietic defects occur in the same individuals, although occasionally individual embryos will exhibit only one of the described phenotypes. One explanation for these phenotypes is that *cx43*-morphant embryos are simply delayed in their development. We do not believe this to be the case since the primary indicator of delay is overall size, and the morphant embryos are similarly sized as wild-type injected embryos (or unaffected embryos from the same clutch). Individuals affected for heart development exhibit pronounced pericardial edema as early as 50–60 hpf. Closer examination of the heart in these animals reveals defects in heart morphology including partial or complete defects in folding (Fig. 4). To assess the hematopoietic phenotype, MO-injected embryos were stained for globin using *o*-dianisidine. By 72 hpf, red blood cells (RBCs) are normally observed streaming over the yolk, progressing towards the heart. In *cx43*-MO-injected embryos, there is significant reduction in the number of RBCs in circulation (Fig. 4). The heart and blood phenotypes in zebrafish are strikingly similar to the

Table 4
cx43-MO injections in wild-type and sof^{b123} embryos

Genotype	MO (ng injected)	Percent (%)				
		WT	MO	NS	Death	*n*
wild-type	standard (1.5 ng)	97	2	1	0	94
wild-type	cx43 (1.5 ng)	23	42	6	29	111
wild-type	cx43 (0.25 ng)	85	5	2	8	143
sof^{b123}/sof^{b123}	cx43 (0.25 ng)	29	48	7	16	248

The total number of scored animals (*n*) include only the embryos that were healthy at 24 h after injection. Phenotypes were scored at 3 dpf and were separated into four mutually exclusive categories: WT (normal), MO (for *cx43*-MO-specific phenotypes), NS (non-specific), and death (after initial 24 h). *cx43*-MO specific phenotypes are not mutually exclusive, and include defects in blood, heart, and eye (see text). Non-specific phenotypes are phenotypes that occur in all populations after injection of either morpholino. These include anterior and/or posterior truncations and CNS necrosis.

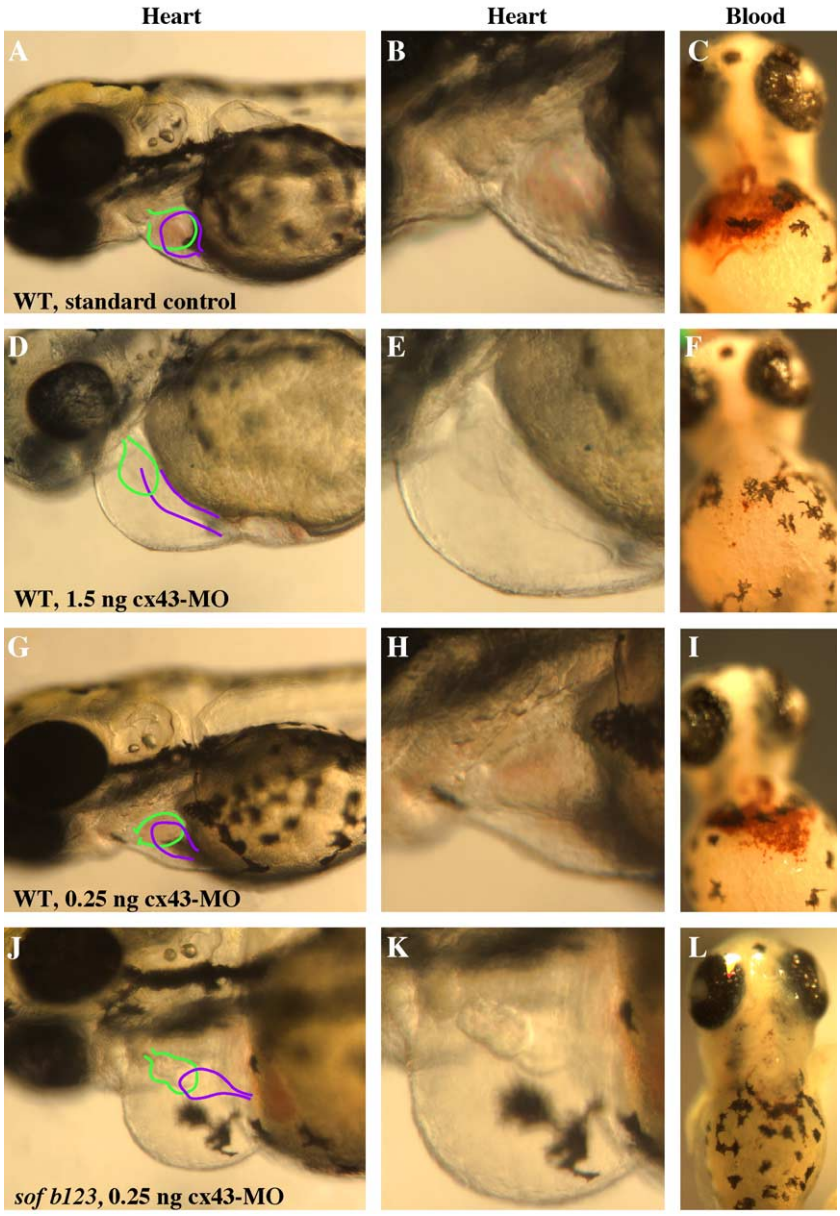

Fig. 4. *cx43*-MO injections cause defects in heart morphology and hematopoiesis. Representative photographs of each morpholino injection trial are shown. (A–C) Wild-type embryos injected with 1.5 ng of standard control morpholino. (D–F) Wild-type embryos injected with 1.5 ng of *cx43*-MO. (G–I) Wild-type embryos injected with 0.25 ng of *cx43*-MO. (J–L) sof^{b123} embryos injected with 0.25 ng *cx43*-MO. The left column (heart) shows the heart morphology phenotype at 72 hpf. The atrium is outlined in purple, and the ventricle is outlined in green. The middle column (heart) shows higher magnification views of the hearts in the left column. The right column (blood) shows *o*-dianisidine staining of globin (representing red blood cells) in injected embryos at 72 hpf.

phenotypes observed in the $cx43^{-/-}$ knockout mice, confirming that the loss of zebrafish *cx43* exerts conserved roles during vertebrate development. It is therefore unlikely that embryos completely lacking zebrafish *cx43* would survive beyond embryogenesis.

Considering the above analysis of *cx43* gene knockdown, we anticipate that complete loss of *cx43* function (i.e., a null allele) would be lethal. However, since none of our non-complementing alleles of *cx43* results in lethality, we suggest that each ENU-induced allele that we identified may also be hypomorphic. Indeed, no decrease in viability was observed among any of our *sof* alleles (not shown). One possibility is that a null allele would be lethal in trans-heterozygous combination with sof^{b123}, thereby preventing the recovery of null alleles from our non-complementation screen.

To determine if sof^{b123} embryos exhibit increased sensitivity to the *cx43*-MO, we first identified a dose of *cx43*-MO that would not elicit phenotypes in wild-type embryos. Injection of 0.25 ng of *cx43*-MO was ineffective in causing phenotypes in wild-type embryos (Table 4). In contrast, injection of the lower amount in sof^{b123} embryos results in a range of phenotypes essentially identical to that observed for the higher dose in wild-type embryos (Table 4 and Fig. 4). These data

provide further evidence that the *cx43* gene is partially abrogated in *sof*^{b123} mutants. Furthermore, this result demonstrates the specificity of the *cx43*-MO and supports our previous conclusion that *cx43* is the mutated gene in *sof*^{b123}.

In light of the observed *cx43*-morpholino phenotypes, it is of interest to consider when *cx43* function is required. Since *cx43* is expressed in the heart both before (Chatterjee et al., 2001) and during the appearance of heart phenotypes (Fig. 3D), it is not clear when *cx43* function is required for proper heart development. For example, *cx43* function may be required early in development for the occurrence of later event(s), *cx43* function may be required at the time that we observe the morphant phenotypes, or *cx43* function may be required throughout this time. Further analyses of the progression of the *cx43* morphant phenotypes in combination with the expression of additional markers for heart development (and blood development) are in progress and will be described elsewhere.

A model for how cx43 may regulate segment length

A central question in development is how animals regulate the size of tissues. In this report, we identify one potential mechanism based on our analysis of the *sof*^{b123} mutant, which develops short bony segments during fin growth. This phenotype is caused by mutations in the *cx43* gene, whose gene product is responsible for local cell–cell communication via the formation of gap junctions. Expression of *cx43* is observed distally in a crescent, laterally as cells which flank the germinal compartment of cell division, and more proximally around newly forming joints. We favor a model by which the lateral expression domain acts as a biological ruler. Thus, we suggest that the lateral cells communicate via Cx43-gap junctions by the intercellular diffusion of small molecules. This model posits a source of small molecule at one end, perhaps the more proximal (newly formed) joint. The addition of cells distal to the joint causes the concentration of the critical small molecule to be decreased. This reduced concentration may function as a signal instructing the precursors of joint cells (i.e., *cx43*-expressing cells in the distal crescent) to differentiate, thus capping the newly formed segment with *cx43*-positive joint cells. In *sof* mutants, the function of Cx43-gap junctions is likely compromised. We speculate that the critical gap junction permeable molecule is inefficiently distributed among the lateral cells. This critical molecule therefore appears to achieve its low concentration prematurely, and as a consequence halts segment growth.

A prediction of the described model is that *sof* mutants add segments with higher frequency than wild-type fins. However, we have previously found this not to be the case. Rather, *sof* mutants add segments at a similar rate as wild-type (Iovine and Johnson, 2000). This observation does not exclude the possibility that gap junctional intercellular communication through *cx43*-gap junctions exhibits a measuring function. We must consider that gap junctional communication regulates an additional (or a different) process required for normal segment length. Therefore, we decided to examine cell proliferation in wild-type and *sof* fins. We labeled 8-week-old zebrafish with the thymidine analog bromo-deoxy-uridine (BrdU), and subsequently processed caudal fins for BrdU incorporation. We find that *sof* fins consistently contain fewer labeled cells than wild-type fins (Fig. 5), revealing that cell proliferation is indeed affected in *sof* mutants. At least two possibilities reconcile these data with the observed expression of *cx43* at the distal ends of growing fin rays. One possibility is consistent with the model presented above (i.e., that *cx43*-expressing osteoblasts are derived from the *cx43*-expressing cells of

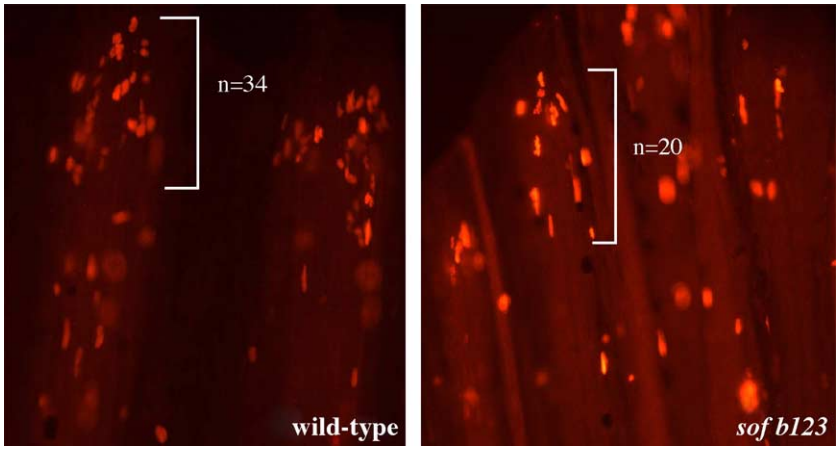

Fig. 5. Cell proliferation during ontogenetic growth in wild-type and *sof*^{b123} caudal fins. Wild-type and *sof*^{b123} fish were labeled with BrdU for 6 h. BrdU-positive cells are labeled in red. The bracket indicates the region from which cells were counted, n indicates the number of BrdU-positive cells in this particular fin ray (note: all BrdU-positive cells are not in this focal plane). Left: wild-type fin ray showing BrdU-labeled cells. On average, 32 ± 5 cells are labeled in the third fin ray from either lobe (n = 10 fins). Right: *sof*^{b123} fin ray showing BrdU-labeled cells. On average, 21 ± 3 cells are labeled in the third fin ray from either lobe (n = 10 fins).

the distal crescent). In this scenario, the *cx43*-expressing cells in lateral positions may regulate both osteoblast differentiation and cell proliferation coordinately. The second possibility favors an alternate model, where the *cx43*-expressing cells of the distal crescent and the differentiated osteoblasts represent independent populations of *cx43*-expressing cells. If this model is correct, then *cx43*-expressing cells in the lateral positions may regulate cell proliferation in the germinal compartment, rather than regulating osteoblast differentiation. Distinguishing between these possibilities will require further analysis of *cx43* expression together with markers for osteoblast precursors and cell proliferation.

Conclusions

Our interest in *cx43* results from our finding that the sof^{b123} phenotype is caused by mutations in *cx43*. This conclusion is supported by three lines of evidence: the sof^{b123} mutation maps to the *cx43* gene, the expression of *cx43* is significantly reduced in sof^{b123} animals, and ENU-induced alleles of *sof* have mutations in the *cx43* coding sequence. While it is currently not possible to phenocopy adult phenotypes using morpholino technology, we induced *cx43*-MO phenotypes in sof^{b123} embryos by injecting a limiting dose of *cx43*-MO. Thus, we have demonstrated by expression and by functional analyses that sof^{b123} embryos are compromised for *cx43* production, providing strong support for the molecular identification of *sof* as *cx43*. Furthermore, we have shown that the expression and function of *cx43* is conserved in zebrafish by assaying gene expression in situ and by completing *cx43* knockdown experiments.

This work identifies the first molecular identification of a fin length mutation (*sof*) as well as the first connexin mutations in zebrafish, and thereby identifies local cell–cell communication as a potential mechanism for the regulation of tissue size. Defects in gap junctional communication have been correlated with the dysregulation of growth control, although little is known about the molecular nature of the events that occur downstream of GJIC (Mesnil, 2002). Identification of viable alleles of *cx43* in a genetically tractable vertebrate now provides additional opportunities to understand the nature of these signaling events. Indeed, a comprehensive understanding of many signaling mechanisms has been greatly enhanced by their presence in yeast, fruit flies, and nematodes, where powerful forward genetic approaches can be applied to find interacting components of molecular pathways. The connexin gene family appears to be an innovation specific to the chordates (Sasakura et al., 2003) and it is therefore not possible to utilize invertebrate animals to identify downstream molecular interactions. As demonstrated by the enhanced sensitivity of sof^{b123} to the *cx43*-MO, sof^{b123} mutants provide a sensitized genetic background for forward genetic analysis to find genes that interact with *cx43*, possibly including the targets of connexin signaling responsible for regulation of bone morphology and growth.

Acknowledgments

The authors would like to thank Matthias Falk, Lynne Cassimeris, Alex Brands, and Mirella Bucci for critical reading of this manuscript, and Tamra Mendelson for assistance with the PAUP analysis. We thank Jake Fugazzotto for cryosectioning. Colleen Boggs and Jake Fugazzotto for maintain and care the zebrafish colonies. This work was supported by the NIDCR (MKI-5K22DE014863), the Bioengineering and Bioscience 2020 Funds (MKI), and the NICHD (SLJ-HD08536).

Appendix A. Supplementary data

Supplementary data associated with this article can be found, in the online version, at doi:10.1016/j.ydbio.2004.11.005.

References

Bao, X., Altenberg, G.A., Reuss, L., 2004. Mechanism of regulation of the gap junction protein connexin 43 by protein kinase C-mediated phosphorylation. Am. J. Physiol.: Cell Physiol. 286, C647–C654.

Bergoffen, J., Scherer, S.S., Wang, S., Scott, M.O., Bone, L.J., Paul, D.L., Chen, K., Lensch, M.W., Chance, P.F., Fischbeck, K.H., 1993. Connexin mutations in X-linked Charcot-Marie-Tooth disease. Science 262, 2039–2042.

Borday, V., Thaeron, C., Avaron, F., Brulfert, A., Casane, D., Laurenti, P., Geraudie, J., 2001. evx1 transcription in bony fin rays segment boundaries leads to a reiterated pattern during zebrafish fin development and regeneration. Dev. Dyn. 220, 91–98.

Chatterjee, B., Li, Y.X., Zdanowicz, M., Sonntag, J.M., Chin, A.J., Kozlowski, D.J., Valdimarsson, G., Kirby, M.L., Lo, C.W., 2001. Analysis of Cx43alpha1 promoter function in the developing zebrafish embryo. Cell Commun. Adhes. 8, 289–292.

Chatterjee, B., Meyer, R.A., Loredo, G.A., Coleman, C.M., Tuan, R., Lo, C.W., 2003. BMP regulation of the mouse connexin43 promoter in osteoblastic cells and embryos. Cell Commun. Adhes. 10, 37–50.

Cheng, S., Christie, T., Valdimarsson, G., 2003. Expression of connexin48.5, connexin44.1, and connexin43 during zebrafish (*Danio rerio*) lens development. Dev. Dyn. 228, 709–715.

Detrich III, H.W., Kieran, M.W., Chan, F.Y., Barone, L.M., Yee, K., Rundstadler, J.A., Pratt, S., Ransom, D., Zon, L.I., 1995. Intraembryonic hematopoietic cell migration during vertebrate development. Proc. Natl. Acad. Sci. U. S. A. 92, 10713–10717.

Goldsmith, M.I., Fisher, S., Waterman, R., Johnson, S.L., 2003. Saltatory control of isometric growth in the zebrafish caudal fin is disrupted in long fin and rapunzel mutants. Dev. Biol. 259, 303–317.

Goss, R.J., Stagg, M.W., 1957. The regeneration of fins and fin rays in *Fundulus heteroclitus*. J. Exp. Zool. 136, 487–507.

Haas, H.J., 1962. Studies on mechanisms of joint and bone formation in the skeleton rays of fish fins. Dev. Biol. 5, 1–34.

Hukriede, N., Fisher, D., Epstein, J., Joly, L., Tellis, P., Zhou, Y., Barbazuk, B., Cox, K., Fenton-Noriega, L., Hersey, C., Miles, J., Sheng, X., Song, A., Waterman, R., Johnson, S.L., Dawid, I.B.,

Chevrette, M., Zon, L.I., McPherson, J., Ekker, M., 2001. The LN54 radiation hybrid map of zebrafish expressed sequences. Genome Res. 11, 2127–2132.

Iovine, M.K., Johnson, S.L., 2000. Genetic analysis of isometric growth control mechanisms in the zebrafish caudal Fin. Genetics 155, 1321–1329.

Johnson, S.L., Gates, M.A., Johnson, M., Talbot, W.S., Horne, S., Baik, K., Rude, S., Wong, J.R., Postlethwait, J.H., 1996. Centromere-linkage analysis and consolidation of the zebrafish genetic map. Genetics 142, 1277–1288.

Kelsell, D.P., Dunlop, J., Stevens, H.P., Lench, N.J., Liang, J.N., Parry, G., Mueller, R.F., Leigh, I.M., 1997. Connexin 26 mutations in hereditary non-syndromic sensorineural deafness. Nature 387, 80–83.

Landis, W.J., Geraudie, J., 1990. Organization and development of the mineral phase during early ontogenesis of the bony fin rays of the trout *Oncorhynchus mykiss*. Anat. Rec. 228, 383–391.

Lecanda, F., Warlow, P.M., Sheikh, S., Furlan, F., Steinberg, T.H., Civitelli, R., 2000. Connexin43 deficiency causes delayed ossification, craniofacial abnormalities, and osteoblast dysfunction. J. Cell Biol. 151, 931–944.

Mari-Beffa, M., Carmona, M.C., Becerra, J., 1989. Elastoidin turn-over during tail fin regeneration in teleosts. A morphometric and radioautographic study. Anat. Embryol. (Berl.) 180, 465–470.

Mesnil, M., 2002. Connexins and cancer. Biol. Cell 94, 493–500.

Montecino-Rodriguez, E., Dorshkind, K., 2001. Regulation of hematopoiesis by gap junction-mediated intercellular communication. J. Leukocyte Biol. 70, 341–347.

Nasevicius, A., Ekker, S.C., 2000. Effective targeted gene 'knockdown' in zebrafish. Nat. Genet. 26, 216–220.

Nechiporuk, A., Keating, M.T., 2002. A proliferation gradient between proximal and msxb-expressing distal blastema directs zebrafish fin regeneration. Development 129, 2607–2617.

Paznekas, W.A., Boyadjiev, S.A., Shapiro, R.E., Daniels, O., Wollnik, B., Keegan, C.E., Innis, J.W., Dinulos, M.B., Christian, C., Hannibal, M.C., Jabs, E.W., 2003. Connexin 43 (GJA1) mutations cause the pleiotropic phenotype of oculodentodigital dysplasia. Am. J. Hum. Genet. 72, 408–418.

Poss, K.D., Shen, J., Nechiporuk, A., McMahon, G., Thisse, B., Thisse, C., Keating, M.T., 2000. Roles for Fgf signaling during zebrafish fin regeneration. Dev. Biol. 222, 347–358.

Rawls, J.F., Johnson, S.L., 2000. Zebrafish kit mutation reveals primary and secondary regulation of melanocyte development during fin stripe regeneration. Development 127, 3715–3724.

Rawls, J.F., Frieda, M.R., McAdow, A.R., Gross, J.P., Clayton, C.M., Heyen, C.K., Johnson, S.L., 2003. Coupled mutagenesis screens and genetic mapping in zebrafish. Genetics 163, 997–1009.

Reaume, A.G., de Sousa, P.A., Kulkarni, S., Langille, B.L., Zhu, D., Davies, T.C., Juneja, S.C., Kidder, G.M., Rossant, J., 1995. Cardiac malformation in neonatal mice lacking connexin43. Science 267, 1831–1834.

Sasakura, Y., Shoguchi, E., Takatori, N., Wada, S., Meinertzhagen, I.A., Satou, Y., Satoh, N., 2003. A genomewide survey of developmentally relevant genes in *Ciona intestinalis*: X. Genes for cell junctions and extracellular matrix. Dev. Genes Evol. 213, 303–313.

Shiels, A., Mackay, D., Ionides, A., Berry, V., Moore, A., Bhattacharya, S., 1998. A missense mutation in the human connexin50 gene (GJA8) underlies autosomal dominant "zonular pulverulent" cataract, on chromosome 1q. Am. J. Hum. Genet. 62, 526–532.

Shimoda, N., Knapik, E.W., Ziniti, J., Sim, C., Yamada, E., Kaplan, S., Jackson, D., de Sauvage, F., Jacob, H., Fishman, M.C., 1999. Zebrafish genetic map with 2000 microsatellite markers. Genomics 58, 219–232.

Sohl, G., Willecke, K., 2004. Gap junctions and the connexin protein family. Cardiovasc. Res. 62, 228–232.

Swofford, D.L., 2000. PAUP*, Phylogenetic Analysis Using Parsimony (*and Other Methods). Sinauer Associates, Sunderland, MA.

Westerfield, M., 1993. The Zebrafish Book: A guide for the laboratory use of zebrafish (*Brachydanio rerio*). University of Oregon Press, Eugene, OR.

White, T.W., 2003. Nonredundant gap junction functions. News Physiol. Sci. 18, 95–99.